Sampling-dependent systematic errors in effective harmonic models

E. Metsanurk and M. Klintenberg

Phys. Rev. B **99**, 184304 — Published 28 May 2019

DOI: 10.1103/PhysRevB.99.184304

Sampling dependent systematic errors in effective harmonic models

E. Metsanurk* and M. Klintenberg
Department of Physics and Astronomy, Uppsala University, Box 516, S-75120 Uppsala, Sweden
(Dated: April 25, 2019)

Effective harmonic methods allow for calculating temperature dependent phonon frequencies by incorporating the anharmonic contributions into an effective harmonic Hamiltonian. The systematic errors arising from such an approximation are explained theoretically and quantified by density functional theory based numerical simulations. Two techniques with different approaches for sampling the finite temperature phase space in order to generate the force-displacement data are compared. It is shown that the error in free energy obtained by using either can exceed that obtained from 0 K harmonic lattice dynamics analysis which neglects the anharmonic effects.

I. INTRODUCTION

The harmonic approximation of the potential energy is a fundamental part of the analysis of vibrational properties of materials both in theoretical and experimental studies [1]. Its usefulness is multifold in the sense that not only does it allow for capturing the dominant part of the potential energy surface, but makes possible to derive exact analytical relations for all temperature dependent vibrational thermodynamic properties. In addition, the harmonic system can be used as a reference point for either integration- or perturbation-based methods in order to find the corrections due to anharmonicity that always exists in real systems.

The lattice dynamics approach [2] to calculate the normal vibrational modes of a crystal can break down when either very strong quantum mechanical effects dominate as is the case for crystalline helium [3] or more commonly due to mechanical instabilities, for example cubic zirconia [4] or titanium, zirconium and hafnium in BCC structure [5]. This results in some of the normal modes having imaginary vibrational frequencies due to decrease in the total potential energy when the atoms are displaced along those modes. Since the harmonic free energy and all the other derived thermodynamic properties are defined as integrals over the whole normal mode space, it would result in complex-valued properties and are, thus, commonly interpreted as undefined.

Recently, methods have been proposed to calculate free energies of such systems both for cases where the lattice is dynamically unstable [6] or stabilized due to temperature [7]. Both are based on partitioning of atomic configuration space, calculating the free energy of each region separately and adding those together consistent with equilibrium thermodynamics.

Instead of the aforementioned detailed mapping it is also possible to fit high temperature force-displacement data obtained from atomistic simulation to a truncated expansion of the potential energy surface after which the second order effective force constants can be used to calculate the temperature dependent phonon frequencies and, hence, the effective harmonic free energy. This is the basis for the methods of self-consistent *ab-initio* lattice dynamics (SCAILD) [5, 8, 9] and temperature-dependent effective potential (TDEP) [10–12]. Neither are inherently limited to be used for analyzing only systems with dynamical instabilities, which could be considered as the most severe case, but any kind of anharmonicity.

Currently the best way to gather the data for either of the methods is through density functional theory (DFT) [13] which in principle provides a parameter-free way to explore the dynamics of realistic, as opposed to model, systems. *Ab-initio* based thermodynamics has been shown to be a promising way to predict the thermal properties of materials taking all the relevant excitations, not limited to vibrational, into account [14, 15].

Without considering whether DFT with its approximations can provide reliable enough data, there are also other systematic and statistical uncertainties associated with calculating thermodynamic properties. Some of those, such as the limited system size, can be partially dealt by Fourier interpolating the information about vibrations in an infinite crystal [4], while others such as limited amount of time for sampling can be dealt with by upsampled thermodynamic integration with Langevin dynamics (UP-TILD) or harmonically mapped averaging [16, 17]. Regardless of the method used, the total uncertainty required to produce satisfactory results is often under 1 meV/atom. For example, a 6 meV/atom shift on the energy scale results in 400 K (60%) overestimation of the FCC to BCC transition temperature for calcium using *ab-initio* calculations [18].

Given the requirement of high accuracy for any method used to calculate thermodynamic properties it is necessary to understand how the models behave under certain conditions. In this study we analyze the accuracy of effective harmonic models by comparing SCAILD and TDEP both theoretically and numerically at different temperatures. It has been shown that effective harmonic methods do not necessarily give a significant improvement over 0 K harmonic approximation [19] and that the difference between the free energies predicted by the two methods increases with temperature [20], however, no theoretical explanation was provided what in particular could cause the discrepancy between these two very similar models.

* erki.metsanurk@physics.uu.se

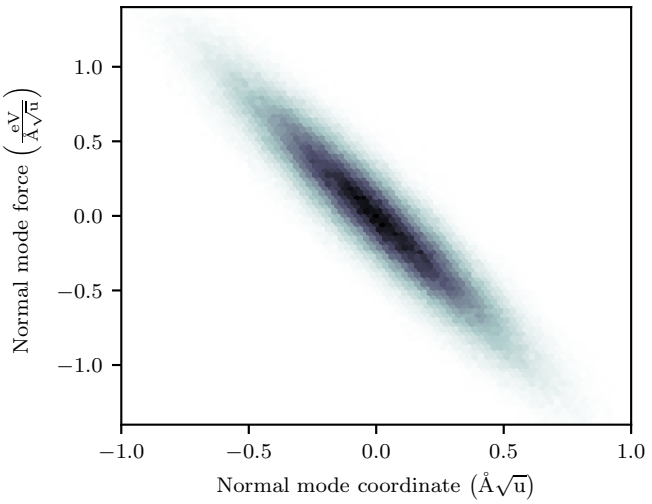

FIG. 1. A histogram of the force-displacement relation for a single phonon mode extracted from a molecular dynamics simulation at 1600 K. The darker areas correspond to higher probability states. A linear fit through the distribution gives the negative square of the effective mode frequency.

II. METHODOLOGY

A. Harmonic approximation at 0 K and finite temperatures

In order to simplify the comparison of the two methods a slight reformulation of the theory is needed compared to that described in the original works. The starting point is the force-displacement relation through a $3N \times 3N$ force constant matrix Φ, so for any atomic configuration c the forces are given by

$$\vec{f_c} = -\Phi(\vec{\theta})\vec{u_c} \tag{1}$$

In a similar fashion to Hellman *et al.* [11], the elements of Φ are expressed as linear combinations of parameters $\vec{\theta}$ as the force constants of crystalline systems are in general not independent, but constrained by rotational, translational and inversion symmetry of the lattice and by the requirement that force appears on any atom under rigid translation of the whole crystal. For the supercell used in this study, the number of force constants are reduced from 82944 to 52.

This allows to rewrite Equation 1 as

$$\vec{f_c} = C(\vec{u_c})\vec{\theta} \tag{2}$$

where the elements of matrix C_c are linear combinations of displacements the coefficients of which depend on the choice of the supercell and the aforementioned symmetry constraints. The parameters $\vec{\theta}$ can now be found with linear least squares method using Moore-Penrose inverse of C

$$\vec{\theta} = C^{+}(\vec{u})\vec{f} \tag{3}$$

Where we have omitted the indices c since both $\vec{f}$ and $\vec{u}$ can contain the forces and displacements of any number of atomic configurations. The more anharmonic the system is, the more configurations are needed in order to keep the uncertainty of the fit sufficiently small. By expressing $\vec{\theta}$ as a function of temperature we obtain a temperature dependent effective harmonic force constant matrix from which the phonon frequencies and eigenvectors can be calculated.

When working only with the vibrational modes commensurate with the supercell it is more convenient to consider the supercell itself to be the unit cell and calculate the exact normal mode frequencies which correspond to $\vec{q} = (0, 0, 0)$, *i.e.* only at the Γ-point of the reciprocal lattice of the supercell. In that case the dynamical matrix for the whole system is

$$D = M^{-\frac{1}{2}}\Phi(\vec{\theta})M^{-\frac{1}{2}} = Q(\vec{\theta})\Omega^2(\vec{\theta})Q^T(\vec{\theta}) \tag{4}$$

where M is a diagonal matrix of the masses of the atoms, Ω^2 a diagonal matrix of eigenvalues and Q a matrix the columns of which are the eigenvectors.

By substituting Equation 4 into Equation 1 we get the following general equation that applies both to SCAILD and TDEP

$$Q^T(\vec{\theta})M^{-\frac{1}{2}}\vec{f_c} = -\Omega^2(\vec{\theta})Q^T(\vec{\theta})M^{\frac{1}{2}}\vec{u_c} \tag{5}$$

One of the approximations of SCAILD is that the eigenvectors are temperature independent and can, thus, be obtained from a quick 0 K phonon calculation. Whether this holds, depends on the symmetry properties of the system and the choice of the supercell, which determines the grid of sampled q-points [21]. For the system considered in this work, this approximation does not have significant effect on the results.

Equation 5 then becomes

$$\vec{\phi_c} = -\Omega^2\vec{v_c} \tag{6}$$

where $\vec{\phi_c} = Q^T M^{-\frac{1}{2}}\vec{f_c}$ is the normal mode force and $\vec{v_c} = Q^T M^{\frac{1}{2}}\vec{u_c}$ the normal mode displacement. The $\vec{\theta}$ dependence is removed since we are interested in Ω, which can be obtained from a simple linear least squares fit, and how its elements are related to the parameters becomes irrelevant.

For a perfectly harmonic crystal there exists one and only one Ω^2. For anharmonic crystals however the uniqueness is lost due to the higher order terms in the Hamiltonian becoming relevant. A typical distribution of the normal mode force-displacement relation for a single phonon mode is depicted in Figures 1 and 3. The shape is that of a Gaussian due to both the nature of

constant temperature sampling of the configurations and the anharmonicity of the system. The modes that are symmetrically equivalent can be placed on the same plot thereby increasing the amount of data, thereby reducing the uncertainty of the linear fit and retaining the symmetry properties of the vibrations.

As we have shown, TDEP is mathematically equivalent to SCAILD for systems with temperature independent phonon eigenvectors. The linear least squares fit is done in real space for the former and in normal mode space for the latter.

Our approach differs slightly from the original formulation of SCAILD where sampling of the normal mode displacements, in order to obtain the forces, was limited to certain discrete values that give the same mean squared displacement as a quantum harmonic oscillator at a constant temperature, *i.e.*

$$\vec{u} = M^{-\frac{1}{2}} Q \vec{d} \tag{7}$$

where

$$d_i = \pm \sqrt{\frac{\hbar}{\Omega_{i,i}} \left[\frac{1}{2} + \left(\exp \frac{\hbar \Omega_{i,i}}{k_B T} - 1 \right)^{-1} \right]} \tag{8}$$

That makes it possible to take the average of Ω^2 over all the sampled configurations which means the average slope of all the lines from the origin to every point in the force-displacement plot. This is not mathematically equivalent to a linear least squares fit through all the points. In addition, when the displacements for SCAILD are sampled from a Gaussian distribution, as done in this work, the most likely displacement for a given mode is zero while the force due to the anharmonicity is nonzero which leads to many large positive and negative Ω^2 values which are not likely to cancel out leading to a large error in the estimation of the average value.

B. Sampling of the configuration space

The major difference between TDEP and SCAILD is the way the displacements are obtained. For TDEP it is a constant temperature molecular dynamics simulation consistent with the Hamiltonian of the anharmonic system whereas for SCAILD the displacements are sampled from the distribution self-consistent with the current best fitted harmonic Hamiltonian. The major advantage of the latter is the reduction in the number of calculations due to more efficient generation of uncorrelated samples as there exists an analytical expression that gives correct constant temperature statistics.

Using the samples generated by a canonical molecular dynamics or Monte Carlo simulation can be interpreted as finding the harmonic potential that reproduces the forces given by the anharmonic Hamiltonian for constant temperature with the smallest error in least square sense. It is not unlike using the method of force matching quite commonly employed in order to fit empirical interatomic potentials to DFT reference data [22]. Lack of transferability is often an issue with empirical potentials and, as we explain below, it also plays an important role in the effective harmonic models.

It is slightly less obvious what the sampling used in SCAILD method yields. In addition to the resulting model being harmonic, the displacements themselves are generated assuming non-interacting phonon modes. It has been suggested that this results in probing the wrong parts of the phase space [23] which is certainly true when the actual anharmonic system is concerned, however the goal here is not to perfectly reproduce the whole anharmonic Hamiltonian, but to pack the anharmonic vibrational information into a truncated Taylor expansion of the potential. Nevertheless by careful reasoning one can identify the possible effects of the harmonic sampling when compared to the anharmonic one. Since in the former case all the correlations in the motion of the normal modes are ignored, the probability of sampling higher energy configurations increases which results in larger magnitudes for the sampled forces and in turn higher effective vibrational frequencies which increase with temperature.

While it is clear that the two sampling methods are different, it does not automatically follow that one provides a better free energy estimation than the other. In either case we obtain a harmonic Hamiltonian both of which are just approximations and so are the predicted free energies. While there might exist an effective harmonic model that gives the exact free energy for the system, it is not immediately clear whether either of the methods should do that.

C. Thermodynamic integration and free energy perturbation

Since we expect SCAILD and TDEP to give different harmonic force constant matrices and therefore also different free energies, the full vibrational free energy needs to be calculated for a proper comparison. Both methods provide an excellent reference system for free energy perturbation (FEP) and thermodynamic integration (TI) when compared to the Einstein crystal [24, 25] which has smaller overlap with the phase space of the anharmonic system, or a 0 K harmonic model [26, 27] which has undefined free energy in case of phonon modes with imaginary frequencies. It must be noted that the efficiency of thermodynamic integration can be increased even more by using an intermediate potential, such as local anharmonic [28], semiempirical [29], or one based on machine learning [19].

Both FEP and TI allow to calculate free energy differences from ensemble averages of energy differences. There are several variations of each. In this work we used a linear path through a parameter λ from the effec-

tive harmonic system to the anharmonic one, in our case DFT system as follows:

$$U(\lambda) = \lambda U_{\mathrm{DFT}} + (1-\lambda)U_{\mathrm{EH}} \tag{9}$$

To get the free energy difference from thermodynamic integration we calculate

$$\Delta F = \int_0^1 \left\langle \frac{\partial U(\lambda)}{\partial \lambda} \right\rangle_\lambda d\lambda = \int_0^1 \langle U_{\mathrm{DFT}} - U_{\mathrm{EH}} \rangle_\lambda \, d\lambda \tag{10}$$

In practice there are possibilities either to sample λ on a discrete, but not necessarily equidistant grid or perform adiabatic switching where λ changes continuously throughout the simulation.

Since SCAILD and TDEP sample a lot of configurations and provide both the harmonic and DFT energies, it is also in principle possible to calculate the anharmonic free energy without any extra steps through free energy perturbation.

$$\Delta F = -1/\beta \cdot \ln \langle \exp\left[-\beta(U_B - U_A)\right] \rangle_A \tag{11}$$

For TDEP, U_A are the potential energies from a DFT-MD calculation and U_B the potential energies calculated using the fitted harmonic model. For SCAILD, U_A are the harmonic potential energies calculated using the converged fit and U_B the potential energies for the same structures obtained from DFT. FEP can also be done using stratified calculations. Similarly to thermodynamic integration several intermediate simulations using mixed Hamiltonians of the two endpoints can be done and the free energy differences between each step calculated using Equation 11 and subsequently summed together [30].

D. Calculations

Cubic zirconia was chosen for the system to be studied for several reasons. It has been studied both using 0 K [4], self consistent lattice dynamics [8] and other methods [31]. At ambient pressure it is not dynamically stable as indicated by large amount of imaginary phonon modes which disappear when a SCAILD analysis is performed. Another option for achieving dynamical stability for cubic ZrO2 is to put it under high pressure which we opted to do in order to retain the ability to compute the free energy from 0 K phonon calculation for comparison.

As explained above, the theory simplifies a lot in cases where the eigenvectors can be assumed not to depend on temperature. ZrO2 contains two types of atoms with relatively large difference in atomic weights which should theoretically allow for the possibility of temperature dependent eigenvectors. The size of the supercell was chosen to be $2\times2\times2$ of the conventional unit cell with lattice parameter of 9.7 Å containing a total of 96 atoms. It is not guaranteed to give a converged free energy with respect to the size, but is a good balance between capturing the overall vibrational, both harmonic and anharmonic, behavior while allowing for sufficiently long molecular dynamics simulations.

All phonon calculations were done using phonopy [2] without applying non-analytical term correction. For SCAILD and TDEP our own implementations were used.

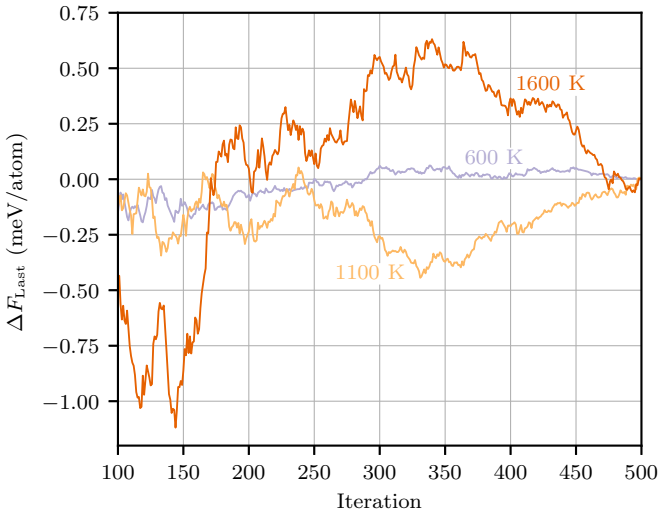

FIG. 2. Convergence of the free energy with respect to the number of iterations using SCAILD. The values are given as a difference to the last step. The free energy difference between two consecutive iterations is typically orders of magnitude smaller than the longer term changes.

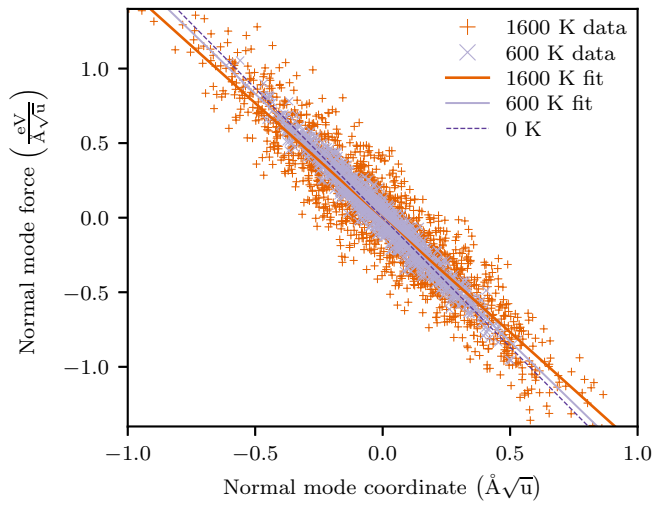

FIG. 3. A typical force-displacement plot for a single frequency but symmetrically equivalent phonon modes for illustrating and fitting effective harmonic models. Not all points are shown for visualization purposes. As the temperature increases the distribution of forces for a fixed displacements broadens. The frequency of the mode is 20.6, 20.1 and 19.4 THz at 0 K, 600 K and 1600 K respectively.

For SCAILD we acquired the eigenvectors from phonopy after which the displacements were generated for every normal mode according to a Gaussian distribution with the same mean square displacement as given by theory for a classical harmonic oscillator at a constant temperature, *i.e.* in Equation 7, $\vec{d}$ is obtained from

$$\sigma_i^2 = \langle d_i^2 \rangle = \frac{k_B T}{\Omega_{i,i}^2} \tag{12}$$

The sampling was from a classical distribution in order to be directly comparable to classical DFT molecular dynamics, although at the investigated temperatures we expect the effect on the results to be relatively small.

As shown in Figure 2 the changes in free energy between consecutive iterations can be orders of magnitude smaller than the changes over many iterations so instead of basing the convergence on the former we ran the simulations for a fixed number of (500) steps.

All the molecular dynamics simulations for TDEP were performed using Nosé-Hoover thermostatting with the Nosé mass corresponding to approximately a time period of 80 fs and velocity Verlet integration with a timestep of 1 fs. The symmetry requirements for the force constant matrix and crystal were taken into account when performing the linear fit of the displacement-force data. No additional cutoff distance in addition to that determined by the supercell was used for the force constants.

For both methods the simulations were done at 600, 1100 and 1600 K. At higher temperatures the oxygen atoms started migrating and occasionally creating vacancy-interstitial pairs which complicates the analysis not only for SCAILD and TDEP, but also for the following thermodynamic integration which set the upper limit used in this work. The number of MD steps was 20000 at 600 and 1100 K, and 30000 at 1600 K.

Thermodynamic integration was done for λ values of 0, 0.1, 0.25, 0.5, 0.75, 0.9 and 1. For TDEP $\lambda = 1$ data is already acquired before the fitting and no extra calculation is needed. The same data was also used for SCAILD at $\lambda = 1$. For SCAILD at $\lambda = 0$ a separate fast MD run was done using the harmonic Hamiltonian after which a subset of uncorrelated samples was chosen for which the energy was calculated using DFT. Whereas Nosé-Hoover thermostat was used for TDEP mostly because it automatically retains the position of the center of mass of the system and therefore simplifies the fitting, Langevin dynamics was used for the thermodynamic integration steps in order to avoid the possibility of incorrect sampling of the phase space when the system is close to harmonic [32]. The drift of the center of mass was not problematic for TI since only the energy differences were obtained instead of displacements.

All DFT calculations were done using VASP [33–36] with projector-augmented wave method [37] with a plane wave cutoff energy of 400 eV and GGA-PBE [38] XC-functional, [39]. The number of electrons treated explicitly was 12 and 6 for Zr and O respectively. A $2 \times 2 \times 2$ Monkhorst-Pack Γ-centered k-point grid [40] and Gaussian smearing with $\sigma = 0.05$ were used.

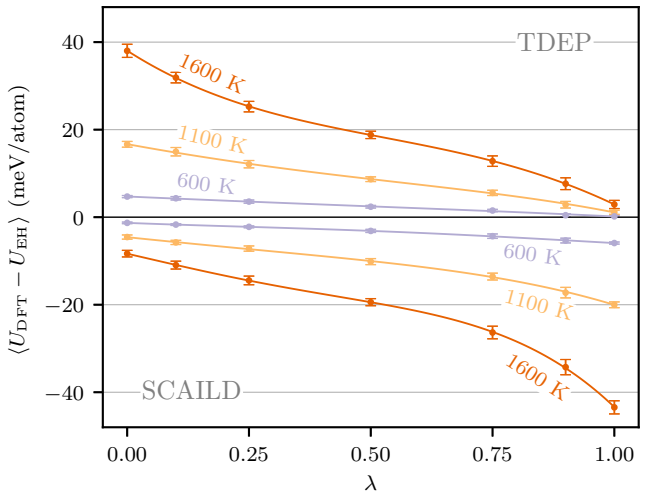

FIG. 4. Thermodynamic integration results for TDEP and SCAILD. Every dot corresponds to one equilibrium MD calculation with a λ-mixed Hamiltonian. The error bars were obtained using block averaging method and are shown for ±3 standard deviations. The continuous line is a 4th order polynomial fit with the reciprocals of the standard deviations used as weights.

The choice for the k-point grid was based on the balance between sufficient accuracy and computational time. Fits for SCAILD and TDEP based on shorter runs with $3 \times 3 \times 3$ Γ-centered grid at 1600 K resulted in roughly 1 meV/atom difference. For thermodynamic integration a check was done by recalculating the $\lambda = 0.5$ point for TDEP at 1600 K using a $4 \times 4 \times 4$ gamma-centered grid. The difference seen was within the statistical uncertainty of the original calculation so no extra up-sampling as done using the UP-TILD [27] method was performed.

As shown by Hellman [23], the relative errors in forces decrease by orders of magnitude as the magnitude of the forces increases to that of the thermally excited states. Based on that the 0 K harmonic calculations including obtaining the eigenvectors for SCAILD were done using a denser $7 \times 7 \times 7$ k-point grid.

III. RESULTS

The vibrational free energies calculated using all of the methods are shown in Table I. The full anharmonic vibrational free energies are in good agreement. Even at the highest considered temperature, 1600 K, all stratified free energy perturbation and thermodynamic integration results are within 1 meV/atom. Both SCAILD and TDEP are however off by about 20 meV/atom and, perhaps surprisingly, even the free energy calculated from harmonic lattice dynamics is a lot closer to the value obtained from thermodynamic integration than those of the either effec-

TABLE I. Vibrational free energies (in meV/atom) calculated by different methods. The meaning of the acronyms is as follows: LD lattice dynamics, H harmonic, EH effective harmonic, AH anharmonic, FEP free energy perturbation, SFEP stratified free energy perturbation, TI thermodynamic integration. For TDEP the EH results are presented both for assuming temperature-independent and temperature-dependent eigenvectors denoted by Q_0 and Q_T respectively.

Method	Type	600 K	1100 K	1600 K
LD	H	4.0	-176.7	-415.9
SCAILD	EH	7.1	-167.3	-398.0
	AH,FEP	4.1	-176.4	-415.1
	AH,SFEP	3.8	-177.9	-419.0
	AH,TI	3.8	-178.1	-419.1
TDEP	EH,Q_0	0.9	-186.8	-438.5
	EH,Q_T	1.0	-186.6	-437.9
	AH,FEP	3.2	-180.1	-422.0
	AH,SFEP	3.4	-177.8	-418.4
	AH,TI	3.5	-177.7	-418.6

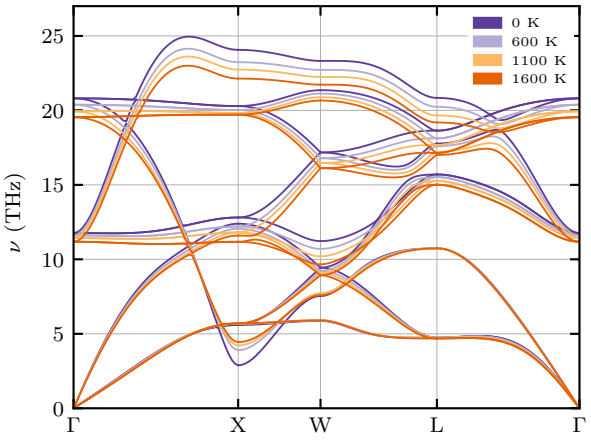

FIG. 5. Phonon dispersion dependence on temperature as predicted by TDEP.

tive harmonic method.

The error in free energies predicted by SCAILD and TDEP is opposite in sign. This is also evident from the thermodynamic integration results shown in Figure 4. Since TDEP force constant matrix is fitted to the DFT-MD results also the average potential energy difference between DFT and TDEP is minimal at $\lambda = 1$. It is also seen that setting the average potential energies to be equal as done in Ref 11 (Equation 21) would do little to reduce the error. In this case the whole TI curve would be shifted down by roughly 3 meV/atom for the temperature of 1600 K which accounts for only 15 % of the total error. Similar conclusions can be drawn for SCAILD for which the agreement with DFT is best at $\lambda = 0$ with the error due to mismatched average potential energies being slightly larger and if taken into account provides a better estimation for the full vibrational free energy than TDEP.

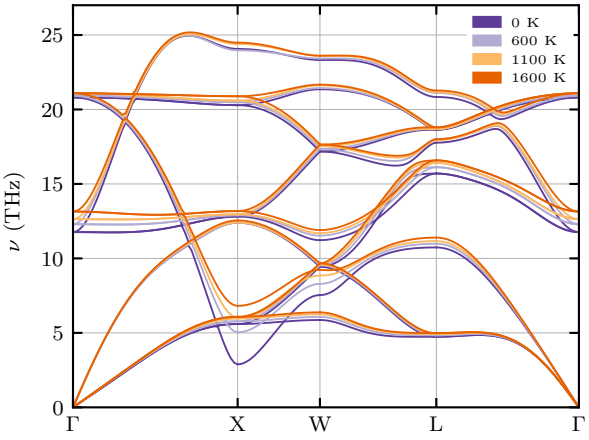

FIG. 6. Phonon dispersion dependence on temperature as predicted by SCAILD.

Free energy perturbation was not able to correct all of the discrepancy possibly due to the limited number of samples, however the stratified version gives free energies that agree very well with TI results. This is expected since the same input data was used for both methods.

In either case shifting the potential energy does not result in change in the force constants and neither in the phonon dispersions which are shown in Figures 5 for TDEP and 6 for SCAILD. The general trend is for TDEP to predict a decrease and for SCAILD an increase in frequencies over all of the reciprocal space. A notable exception to that is the lowest frequency mode at X-point which would be unstable without the external pressure. Both methods predict an increase in the frequency albeit SCAILD from 2.9 THz at 0 K to 6.1 THz, and TDEP to 4.4 THz at 1600 K. The changes in frequencies at high symmetry q-points are depicted in Figure 7. We must note that since the calculations were done at fixed volume, the typical lowering of the frequencies due to thermal expansion is not taken into account.

The reason why TDEP, at least when up to second order force constants are considered, cannot provide a better estimate than SCAILD is that an effective harmonic Hamiltonian fitted at either $\lambda = 0$ or at $\lambda = 1$ exhibits similar non-transferability. Whereas the average energy difference between DFT and EH model can be forced to be zero at one of the endpoints of the TI curve, its absolute value can only monotonically increase as TI is performed and the sampled atomic configurations

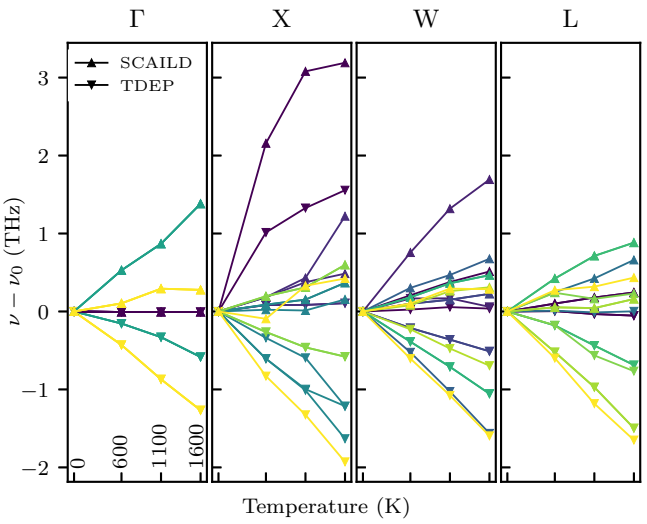

FIG. 7. Temperature dependence of change in phonon mode frequencies at high symmetry points. The darker and lighter colors indicate lower and higher initial frequencies respectively.

will start to differ from those used for the fit. This can be proven using Gibbs-Bogoliubov inequality [41], which states that

$$\left(\frac{\partial^2 F}{\partial \lambda^2}\right)_{NVT} \leq 0 \tag{13}$$

As the anharmonicity increases, the transferability and, thus, the estimate for the full vibrational free energy becomes worse. This can also be explained as follows: let us consider a full infinite expansion of the DFT Hamiltonian. Starting from a harmonic model we carry out the TDEP process, that is perform molecular dynamics runs at $\lambda = 1$, and for each subsequent run increase the number of terms in the expansion. For up to quadratic term the effective harmonic model can be fitted exactly and $\Delta U = 0$ for any λ. As we add more terms ΔU at $\lambda = 0$ starts to deviate from 0 more and more while being kept 0 at $\lambda = 1$. Whereas LD ignores higher than second order terms, both SCAILD and TDEP incorporate those in an effective manner into the harmonic Hamiltonian and as shown, this can lead to a much larger error. In addition, it is not obvious that adding for example the third order force constants to the effective model Hamiltonan necessarily reduces the error, since the second order force constants may remain relatively unaffected.

IV. CONCLUSIONS

Given temperature independent eigenvectors, the effective harmonic models obtained either through SCAILD or TDEP produce two types of systematic errors. One is due to the different choice of the ensemble of displacements and forces used to fit the data. Based on our results neither could be considered better than the other, the reason being that in either case it is not the remaining explicitly anharmonic energy obtained through thermodynamic integration that is minimized, but the potential energy difference at one of the endpoints of the λ-integration curve. The other systematic error, common to both, is introduced by trying to reproduce the anharmonic interactions in an effective harmonic manner.

The free energies predicted by either method diverge as the temperature increases with the general trend being SCAILD predicting an increase in the phonon frequencies and higher free energy than the exact value as opposed to TDEP which predicts decreasing frequencies and lower free energy. For the system considered in this work both give worse estimate of the free energy than 0 K harmonic model. Therefore relying on one or another can introduce large errors when investigating the vibrational thermodynamic properties of materials, especially when the results of either are compared with those obtained through other methods, for example, when using the quasiharmonic approximation to calculate the free energy of one phase, while one of the effective harmonic methods for another, in order to compute the phase stability. In addition, due to the non-linearity of the systematic error with respect to temperature, it is possible that the error in other thermodynamic quantities derived from free energy, such as heat capacity, will have even larger errors. Free energy perturbation can be used without extra computational cost in order to estimate the error, but since it may not account for all of the difference between the approximate and true free energy, thermodynamic integration or any other method that takes all of the anharmonicity explicitly into account has to be used.

V. ACKNOWLEDGMENTS

The research leading to these results has received funding from the Swedish Centre for Nuclear Technology (SKC). Computational resources were provided by Swedish National Infrastructure for Computing (SNIC). Comments by A. Samanta and A. Tamm from LLNL are greatly appreciated.

[1] B. Fultz, Progress in Materials Science **55**, 247 (2010).
[2] A. Togo and I. Tanaka, Scripta Materialia **108**, 1 (2015).
[3] F. W. de Wette, L. H. Nosanow, and N. R. Werthamer, Physical Review **162**, 824 (1967).
[4] K. Parlinski, Z. Q. Li, and Y. Kawazoe, Physical Review Letters **78**, 4063 (1997).
[5] P. Souvatzis, O. Eriksson, M. I. Katsnelson, and S. P. Rudin, Physical Review Letters **100**, 095901 (2008).

[6] A. van de Walle, Q. Hong, S. Kadkhodaei, and R. Sun, Nature communications **6**, 7559 (2015).
[7] S. Kadkhodaei, Q.-J. Hong, and A. van de Walle, Physical Review B **95**, 064101 (2017).
[8] P. Souvatzis and S. P. Rudin, Physical Review B **78**, 184304 (2008).
[9] P. Souvatzis, O. Eriksson, M. I. Katsnelson, and S. P. Rudin, Computational Materials Science **44**, 888 (2009).
[10] O. Hellman, I. A. Abrikosov, and S. I. Simak, Physical Review B **84**, 180301(R) (2011).
[11] O. Hellman, P. Steneteg, I. A. Abrikosov, and S. I. Simak, Physical Review B **87**, 104111 (2013).
[12] I. Mosyagin, O. Hellman, W. Olovsson, S. I. Simak, and I. A. Abrikosov, The Journal of Physical Chemistry A **120**, 8761 (2016).
[13] W. Kohn and L. J. Sham, Phys. Rev. **140**, A1133 (1965).
[14] B. Grabowski, T. Hickel, and J. Neugebauer, physica status solidi (b) **248**, 1295 (2011).
[15] M. Palumbo, B. Burton, A. Costa e Silva, B. Fultz, B. Grabowski, G. Grimvall, B. Hallstedt, O. Hellman, B. Lindahl, A. Schneider, P. E. A. Turchi, and W. Xiong, physica status solidi (b) **251**, 14 (2014).
[16] S. G. Moustafa, A. J. Schultz, and D. A. Kofke, Physical Review E - Statistical, Nonlinear, and Soft Matter Physics **92**, 1 (2015).
[17] S. G. Moustafa, A. J. Schultz, and D. A. Kofke, Journal of Chemical Theory and Computation **13**, 825 (2017).
[18] B. Grabowski, P. Söderlind, T. Hickel, and J. Neugebauer, Physical Review B **84**, 214107 (2011).
[19] B. Grabowski, Y. Ikeda, F. Körmann, C. Freysoldt, A. I. Duff, A. Shapeev, and J. Neugebauer, , 1 (2019).
[20] P. Korotaev, M. Belov, and A. Yanilkin, Computational Materials Science **150**, 47 (2018).
[21] A. A. Maradudin and S. H. Vosko, Reviews of Modern Physics **40**, 1 (1968).
[22] F. Ercolessi and J. B. Adams, Europhysics Letters (EPL) **26**, 583 (1994).
[23] O. Hellman, *Thermal properties of materials from first principles*, Ph.D. thesis (2012).
[24] M. de Koning and A. Antonelli, Physical Review E **53**, 465 (1996).
[25] R. Freitas, M. Asta, and M. de Koning, Computational Materials Science **112**, 333 (2016).
[26] S. Ryu and W. Cai, Modelling and Simulation in Materials Science and Engineering **16**, 085005 (2008).
[27] B. Grabowski, L. Ismer, T. Hickel, and J. Neugebauer, Physical Review B **79**, 134106 (2009).
[28] A. Glensk, B. Grabowski, T. Hickel, and J. Neugebauer, Physical Review Letters **114**, 195901 (2015).
[29] A. I. Duff, T. Davey, D. Korbmacher, A. Glensk, B. Grabowski, J. Neugebauer, and M. W. Finnis, Physical Review B **91**, 214311 (2015).
[30] A. Pohorille, C. Jarzynski, and C. Chipot, The Journal of Physical Chemistry B **114**, 10235 (2010).
[31] M. Sternik and K. Parlinski, The Journal of Chemical Physics **123**, 204708 (2005).
[32] G. J. Martyna, M. L. Klein, and M. Tuckerman, The Journal of Chemical Physics **97**, 2635 (1992).
[33] G. Kresse and J. Hafner, Physical Review B **47**, 558 (1993).
[34] G. Kresse and J. Hafner, Phys. Rev. B **49**, 14251 (1994).
[35] G. Kresse and J. Furthmuller, Comp. Mater. Sci. **6**, 15 (1996).
[36] G. Kresse and J. Furthmüller, Physical review. B, Condensed matter **54**, 11169 (1996).
[37] G. Kresse and D. Joubert, Phys. Rev. B **59**, 1758 (1999).
[38] J. P. J. Perdew, K. Burke, and M. Ernzerhof, Phys. Rev. Lett. **77**, 3865 (1996).
[39] J. P. Perdew, K. Burke, and M. Ernzerhof, Phys. Rev. Lett. **78**, 1396 (1997).
[40] H. Monkhorst and J. Pack, Physical Review B **13**, 5188 (1976).
[41] D. Frenkel, *Understanding Molecular Simulation* (Elsevier, 2002).